Example Solar Electric Propulsion System Asteroid Tours Using Variational Calculus

Roger R. Burrows
NASA Marshall Space Flight Center, Huntsville, Alabama

Exploration of the asteroid belt with a vehicle utilizing a Solar Electric Propulsion System has been proposed in past studies. Some of those studies illustrated multiple asteroid rendezvous with trajectories obtained using approximate methods. Most of the inadequacies of those approximations are overcome in this paper, which uses the calculus of variations to calculate the trajectories and associated payloads of four asteroid tours. The modeling, equations, and solution techniques are discussed, followed by a presentation of the results.

Nomenclature

c = exhaust velocity
$\bar{e}$ = thrust direction unit vector
F = total ion engine thrust
g_0 = gravitational acceleration at Earth's surface
I_{sp} = specific impulse
m = total mass
r = heliocentric radius
$\bar{r}$ = heliocentric radius vector
t = time
v = heliocentric velocity
$\bar{v}$ = heliocentric velocity vector
$\bar{v}_\infty$ = hyperbolic excess velocity vector
λ_m = mass multiplier
λ_v = magnitude of velocity multiplier vector
$\bar{\lambda}_r$ = radius multiplier vector
$\bar{\lambda}_v$ = velocity multiplier vector
μ = sun's gravitational parameter

Subscripts and Superscripts

E = Earth
f = final time
i = at time t_i
T = target
0 = initial time
$(\dot{\ })$ = time derivative
$(\ )^T$ = transpose
$(\ )_i^\pm$ = $\lim(\ )$; $t \to t_i \pm \delta$, $\delta \to 0$, $\delta > 0$

Introduction

FROM the time of the first asteroid discovery in 1801 until the advent of the photographic method in 1892, just over 300 asteroids had been found. Current numbered asteroid catalogs list over 2400 asteroids whose orbits range from preliminary to well determined. In addition, tens of thousands of asteroids brighter than nineteenth magnitude are estimated to exist, vast numbers being less than 1 mi. in diameter.[1] Systematic Earth-based measurements of asteroid physical characteristics—mass, diameter, density, albedo, etc.,—and studies involving multiwavelength spectrophotometry, radiometry, polarimetry, etc., are of great interest to the scientific community for their implications about the early history of the solar system and planetary evolution.[2-5] However, such remote sensing imposes severe constraints on the quality and variety of data obtainable. Scientific instruments making long-term, close-range observations are preferable.

Since the 1960's, scientists and engineers have addressed various aspects of asteroid exploration by instrumented spacecraft.[6-10] The thrust of those studies has converged toward favoring multiple rendezvous with inner and inner main-belt asteroids as the mission mode making the most efficient utilization of launch resources and in-situ science measurements. Chemical propulsion is suitable for multiple-fly-by or single-rendezvous missions.[11-16] but is virtually useless for multiple rendezvous. The only viable current technology that is in a sufficiently advanced state of development is the Solar Electric Propulsion System (SEPS).[17] In point of fact, NASA included an asteroid multiple-rendezvous mission in its 1979 SEPS Request for Proposal (RFP).[18]

The filtering of an asteroid catalog for suitable tour candidates is a formidable task. Finding successive asteroids positioned properly within their orbits so rendezvous can occur sequentially is difficult enough, but the asteroids selected also should represent the broadest possible sampling of asteroid diversity with respect to size, shape, orbit, and composition. The sheer numbers of possible targets dictate very fast approximation techniques be employed to define preliminary tours. Two nonintegrating computational aids, called CHEBYTOP[19] and TOURAST,[20] have been developed for this purpose, and a number of tours satisfying various criteria such as launch dates, flight times, payloads, SEPS vehicle, etc., have been found. This paper takes the sets of asteroids from four of those missions[9,21] and, using slightly different mission scenarios and SEPS vehicle assumptions, uses the calculus of variations (COV) to derive an appropriate set of differential equations which is solved numerically. This process removes most of the approximation and optimality uncertainties associated with the preliminary analytically obtained tours. The numerical problem is highly nonlinear, very sensitive, and, at times, vexing.

Mathematical Formulation and Modeling

The fundamental inertial coordinate system used to define the asteroid orbits and the SEPS vehicle trajectory is a heliocentric, ecliptic system based on the mean equinox and ecliptic of 1950.0 with the sun being the only gravitational source. A combined maximum principle and calculus of variations theory is used to obtain the necessary conditions of optimality.

Submitted Aug. 16, 1983; revision submitted June 13, 1984.

*Aerospace Engineer, Systems Analysis and Integration Laboratory.

Defining state as a seven vector, $\bar{x}^T = (\bar{r}^T, m, \bar{v}^T)$, the basic problem of maximizing the final mass at the last target is formulated in a minimization context:

$$\text{minimize } J = -m_f$$

subject to the differential equations across each transfer arc, $\dot{\bar{x}} = \bar{f}(\bar{x}, t)$, or

$$\dot{\bar{r}} = \bar{v} \tag{1a}$$

$$\dot{m} = -F/c \tag{1b}$$

$$\dot{\bar{v}} = F/m\bar{e} - \mu\bar{r}/r^3 \tag{1c}$$

the rendezvous conditions at each target

$$\bar{r}(t) = \bar{r}_T(t) \tag{2a}$$

$$\bar{v}(t) = \bar{v}_T(t) \tag{2b}$$

and the initial conditions

$$\bar{r}(t_0) = \bar{r}_E(t_0) \tag{3a}$$

$$\bar{v}(t_0) = \bar{v}_E(t_0) + \bar{v}_\infty(t_0) \tag{3b}$$

where

$$F = 2P_b/c \tag{4a}$$

$$c = g_0 I_{sp} \tag{4b}$$

P_b, the total power in the beam of the ion engine, is computed as

$$P_b = \eta_{\text{tss}} P_{\text{PPU}} \tag{5}$$

where η_{tss} is the total efficiency of the thrust subsystem; and P_{PPU} the total power into the PPU's (power processing units).

The power available from the solar array is defined as

$$P_{\text{avail}} = \eta_a P_0 P'(r) - P_{\text{hkp}} \tag{6}$$

where η_a is the array efficiency which accounts for power loss in the solar array-PPU interface; P_0 the end-of-life power of the solar array at 1 a.u.; $P'(r)$ the normalized solar array power at heliocentric distance r; and P_{hkp} the housekeeping power to run heaters, communication equipment, etc., and not available to the thrust subsystem.

Finally, the PPU input power is defined as

$$\begin{aligned} P_{PPU} &= P_{\text{avail}} && \text{if } P_{\min} < P_{\text{avail}} < P_{\max} \\ P_{PPU} &= P_{\max} && \text{if } P_{\text{avail}} \geq P_{\max} \\ P_{PPU} &= 0 && \text{if } P_{\text{avail}} \leq P_{\min} \end{aligned} \tag{7}$$

where

$$P_{\max} = 7(3096) = 21672 \text{ W}$$

$$P_{\min} = 2(1286) = 2572 \text{ W}$$

The normalized performance of the solar array as released in the industry RFP is tabulated in Table 1. These data were fit as a real Laurent series whose form and coefficients are also shown in Table 1. This analytic form peaks at $r = 0.87$ a.u., where $P/P_0 = 1.0742$. A comparison of the tabular data and the fit is shown in Fig. 1. This flat array consists of more than 280,000 solar cells in two wings. The individual silicon cells are 12.8% efficient, 8 mil × 8 cm in size with a 6 mil cover glass, and a resistivity of 2Ω-cm. Undegraded array output is 31.62 kW at 1 a.u.

Table 2 presents the SEPS vehicle assumptions. Degradation of the solar array due to charged particles, cover glass darkening, contamination, etc., is modeled for all time by degrading its output 20%. Calibration coasts and unplanned downtime of 1 day/month were estimated as another 3% power decrease giving a total array degradation of 23% and an end-of-life power of 24.35 kW. This all-at-once degradation method yields conservative payload results.

The PPU/thruster technology assumed in Table 2 is for a 30-cm-diam mercury ion bombardment engine.[22] It is not modeled to the extent that current and voltage set points are determined. Instead, I_{sp} and η_{tss} are held constant and the engine switching strategy indicated in Table 2 is used to track the solar array power along the trajectory. Past comparisons with studies using more detailed engine modeling, optimizing the number of engines firing according to the maximum principle, have shown this approach using the numerical values in Table 2 to be slightly conservative, but highly representative, and less costly in computer time.

The SEPS vehicle is to be stacked on top of a two-stage Inertial Upper Stage (IUS) and carried into low-Earth orbit in the cargo bay of a Space Shuttle with a 65,000 lb payload capability. The IUS payload capability for escape missions is shown in Table 3. These data were quadratically curve fit in two ranges as shown for use in the COV program.

Table 1 Normalized solar array performance and fit

Distance from sun, a.u.	P/P_0	Distance from sun, a.u.	P/P_0
1.0	1.000	2.6	0.224
1.2	0.814	2.8	0.190
1.4	0.660	3.0	0.162
1.6	0.539	3.2	0.138
1.8	0.446	3.4	0.118
2.0	0.372	3.6	0.102
2.2	0.313	3.8	0.088
2.4	0.265	4.0	0.075

Fit: $P' = P(r)/P_0 = \sum_{i=1}^{5} a_i r^{-(i+3)/2}$

Coefficients: $a_1 = -15.603$, $a_2 = 81.164$, $a_3 = -141.08$
$a_4 = 107.3$, $a_5 = -30.781$

Restriction: $r < 0.87$, $P' = 1.0742$

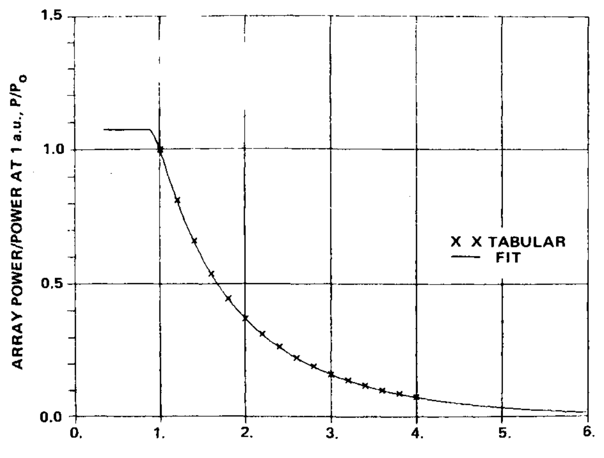

Fig. 1 Normalized solar array characteristics.

The modeling is completed with Table 4 which gives the ephemerides of the tour asteroids as well as some of their physical characteristics.

Defining the multiplier as a seven vector $\bar{\Lambda}^T = (\bar{\lambda}_r^T, \lambda_m, \bar{\lambda}_v^T)$, the COV Euler-Lagrange equations are

$$\dot{\bar{\lambda}}_r = [(\lambda_v/m - \lambda_m/c)A - 3\mu\bar{r}^T\bar{v}/r^5]\bar{r} + \mu\bar{\lambda}_v/r^3 \tag{8a}$$

$$\dot{\lambda}_m = 2P_b\lambda_v/(cm^2) \tag{8b}$$

$$\dot{\bar{\lambda}}_v = -\bar{\lambda}_r \tag{8c}$$

where

$$A = (\eta_{\text{tss}}P_0/c)\sum_{i=1}^{5}(i+3)a_i r^{-(i+7)/2} \tag{8d}$$

The maximum principle and the COV also yield

$$\bar{e} = \bar{\lambda}_v/\lambda_v \tag{9a}$$

$$\bar{v}(t_0) = \bar{v}_E(t_0) + v_{\infty_0}\bar{e}(t_0) \tag{9b}$$

$$\lambda_m(t_f) = 1 \tag{9c}$$

Table 2 SEPS vehicle assumptions

Solar array (flat)
- P_0 (beginning of life) = 31.62 kW
- P_0 (end of life) = 24.35 kW
- P/P_0: Per the industry RFP, July 1979
- Power loss in solar array-PPU interface = 1% = $1 - \eta_a$

Thrust subsystem
- PPU/thruster complement:
  - Carried: 8
  - Thrusting: 7 maximum; 2 minimum
  - Switching: Engines switched one at a time to match PPU input power using fewest engines possible.
- Power per PPU/thruster:
  - Maximum: 3096 W at 2 A
  - Minimum: 1286 W at 1 A

I_{SP} = 3000 s, held constant
η_{tss} = 0.604, held constant
Propellant corresponding to 30,000 A-h lifetime per engine for eight engines = 1945-2199 kg

Mass
- SEPS dry mass = 1450 kg
- Propellant reserves and contingencies = 100 kg
- Trapped propellant = 20 kg

Miscellaneous
- Housekeeping power = P_{hkp} = 1000 W
- IUS/SEPS adapter = 100 kg

Table 3 Two-stage IUS escape payload capability[a]

V_{∞_0}, km/s	IUS payload, kg
0.0	4611
1.0	4472
2.0	4085
3.1623	3420
4.4721	2559

Fit: $m_0 = b_0 + b_1 v_{\infty_0} + b_2 v_{\infty_0}^2$
Coefficients: $0 < v_{\infty_0} \le 2.0$: $b_0 = 4611$, $b_1 = -15$, $b_2 = -124$
$2 < v_{\infty_0} \le 4.4721$: $b_0 = 5011.28$, $b_1 = -394.2$, $b_2 = -34.469$

[a]Source: NASA Marshall Space Flight Center, Jan. 1981.

The maximum principle yields a switching function,

$$\text{SWF} = c\lambda_v/m - \lambda_m \tag{10}$$

such that SWF>0 implies the vehicle thrusts and SWF<0 implies the vehicle coasts. COV analysis also shows that after a target rendezvous has been accomplished $\bar{\lambda}_r$ and $\bar{\lambda}_v$ can be freely rechosen to achieve rendezvous with the next target. λ_m is continuous at all corners (junctures of thrusting and coasting arcs). When there is a fixed-time, stationkeeping coast arc with an asteroid, say from time t_1 to time t_2, the following condition must be satisfied:

$$\text{SWF}_1^- \dot{m}_1^- - \text{SWF}_2^+ \dot{m}_2^+ = 0 \tag{11}$$

If the stationkeeping times were optimal, the conditions would be

$$\text{SWF}_1 = \text{SWF}_2 = 0 \tag{12}$$

Generally for the missions looked at, full optimality required shorter stay times than were allowed so Eq. (11) was used. At all other corner points, SWF = 0.

Due to limiting the maximum and minimum numbers of thrusters firing, and because a PPU has a maximum input power limit, all of the power available from the solar array may not be usable. The minimum power constraint occurs at radii exceeding about 3.11 a.u., but was never applicable because none of the asteroid tours go out that far. The upper power constraint can apply near Earth ($r<1.066$ a.u.) and leads to setting $A=0$ in the multiplier equations while the constraint is operable. This comes about because A is proportional to $\partial P'(r)/\partial r$ which equals zero when PPU input power is held constant by electrical means or pointing the array away from the sun.

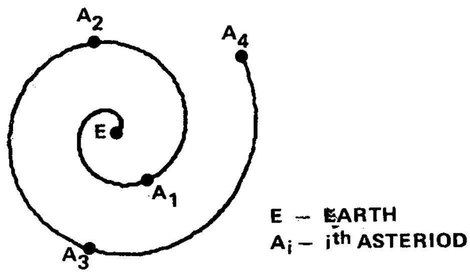

Fig. 2 Notation for asteroid tour.

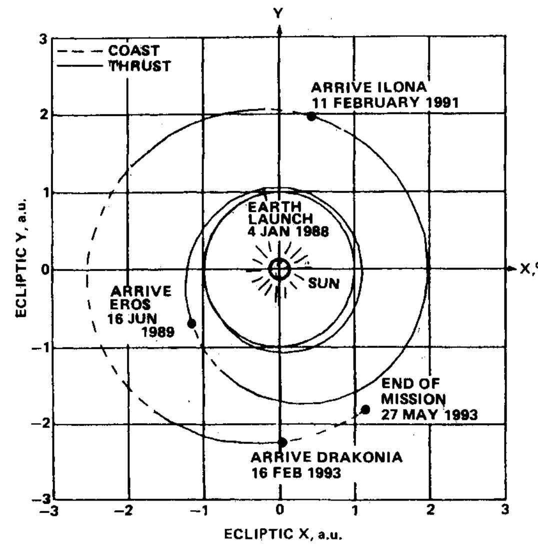

Fig. 3 Eros-Ilona-Drakonia asteroid tour.

Table 4 Physical and orbital characteristics of the Earth and tour asteroids[a]

Type[b]	Name	Radius, km	a, a.u.	e	i, deg	Ω, deg	ω, deg	Period, days	Perihelion date
–	Earth	–	1.0	0.0	0.0	–	–	365.25	–
S	433 Eros	10	1.458	0.223	10.827	303.802	178.478	643.00	Feb. 8, 1982
–	1182 Ilona	9	2.259	0.117	9.398	336.05	62.189	1240.1	Jan. 2, 1984
C,M,E,U	620 Drakonia	17	2.436	0.133	7.714	359.793	334.928	1388.7	April 7, 1982
S	40 Harmonia	59	2.267	0.047	4.257	93.859	268.683	1246.7	Feb. 24, 1984
S	825 Tanina	7	2.226	0.074	3.401	101.07	110.592	1213.0	Oct. 31, 1982
C	19 Fortuna	113	2.442	0.159	1.572	211.049	182.117	1393.8	Nov. 20, 1982
U	4 Vesta	277	2.361	0.090	7.143	103.481	150.276	1325.1	Jan. 21, 1982
E.U	335 Roberta	30	2.473	0.177	5.088	148.005	139.098	1420.45	Aug. 6, 1981
C,M,E,U	201 Penelope	72	2.678	0.181	5.751	156.746	179.972	1600.7	Dec. 2, 1984
U	149 Medusa	13	2.175	0.0654	0.939	159.113	250.501	1171.6	Jan. 3, 1982
E	44 Nysa	34	2.423	0.1498	3.708	131.045	342.092	1377.6	Oct. 20, 1995
C	163 Erigone	36	2.368	0.1918	4.805	159.789	297.339	1331.0	July 11, 1995
S	20 Massalia	70	2.409	0.1439	0.708	– 153.968	255.274	1365.7	Aug. 25, 1995

[a] JPL file – AST*COM – Jan. 26, 1981. [b] C – carbonaceous, S – silicaceous, M – metal rich, E – enstatite, U – unclassifiable.

Table 5 Mission profile for the Eros-Ilona-Drakonia asteroid tour

Julian date – 244,0000	Calendar date	Elapsed time, days	Flight time, days	Event	Propellant drop mass, kg	Mass, kg
7165	1/4/88	0		Launch		4065
7694	6/16/89	529	529	Arrive Eros		3083
			50	Operations at Eros	30	
7744	8/5/89	579		Depart Eros		3053
			545			
8289	2/1/91	1124		Arrive Ilona		2472
			50	Operations at Ilona	30	
8339	3/23/91	1174		Depart Ilona		2442
			696			
9035	2/16/93	1870		Arrive Drakonia		2206
			100	Operations at Drakonia	30	
9135	5/27/93	1970		End of mission		2176

Mass summary

Two-stage IUS capability at $v_{\infty_0} = 1.837$ km/s, kg	4165
IUS-SEPS adapter, kg	– 100
SEPS dry mass, kg	– 1450
Nominal SEPS propellant, kg	– 1889
Reserves + contingencies propellant, kg	– 100
Trapped propellant, kg	– 20
Net payload	606

As a result of the initial mass being a function of v_{∞_0}, λ_m has the initial value

$$\lambda_{m_0} = -\lambda_{v_0} \frac{dm_0}{dv_{\infty_0}} \tag{13}$$

Satisfying the condition for an optimal launch date

$$\bar{\lambda}_{r_0}^T \bar{v}_{\infty_0} - \mathrm{SWF}_0 \dot{m}_0 = 0 \tag{14}$$

caused extreme numerical difficulties, even when launch dates were not far from optimal. Launch date determination is discussed further under solution techniques.

Solution Techniques

The mathematical problem solved is the split boundary value kind. Essentially, for each asteroid, a $\bar{\lambda}_r$, $\bar{\lambda}_v$ set must be found to effect a rendezvous with that asteroid. Whether the SEPS vehicle thrusts or coasts can be determined in either of two ways: 1) the SWF, Eq. (10), is monitored along a trajectory integration and the vehicle thrusts or coasts according to whether SWF > 0 or SWF < 0 or 2) the flight times for a sequence of thrust and coast arcs are postulated, the rendezvous conditions satisfied, and the guessed control sequence is compared with the SWF along the solution trajectory. If they differ, another control sequence is assumed and this process continued until agreement is obtained with the SWF. The second approach is used here since it bypasses instabilities sometimes induced by the first approach in attempting solutions far from converged solutions which cause switching in the wrong order, a lack of switching, or not enough switching.

Numerical solutions are obtained with a simple forward shooting process. For each asteroid, a $\bar{\lambda}_r$, $\bar{\lambda}_v$ set is chosen along with v_{∞_0} and the durations of the thrust and coast arcs. The state and costate are propagated forward and the rendezvous conditions, an appropriate set of SWF's and $\lambda_{m_f} - 1$, are evaluated. If these conditions are not satisfied to some tolerance (eight digits), a version of the generalized secant algorithm[23] is used to vary the independent variables until convergence is attained. Fourth-order Runge-Kutta-Fehlberg formulas[24] for first-order differential equations are used to obtain integration error control which was usually set at four to five digits of accuracy. During coast arcs, state and costate are advanced using a suitable modification of Goodyear's two-body solution.[25]

Table 6 Mission profile for the Harmonia-Tanina-Fortuna asteroid tour

Julian date −244,0000	Calendar date	Elapsed time, days	Flight time, days	Event	Propellant drop mass, kg	Mass, kg
7435	9/30/88	0		Launch		3953
			781			
8216	11/20/90	781		Arrive Harmonia		2982
			50	Operations at Harmonia	30	
8266	1/9/91	831		Depart Harmonia		2952
			636			
8902	10/6/92	1467		Arrive Tanina		2812
			50	Operations at Tanina	30	
8952	11/25/92	1517		Depart Tanina		2782
			517			
9469	4/26/94	2034		Arrive Fortuna		2450
			100	Operations at Fortuna	30	
9569	8/4/94	2134		End of mission		2420

Mass Summary

Two-stage IUS capability at $v_{\infty_0} = 2.059$ km/s, kg	4053
IUS-SEPS adapter, kg	−100
SEPS dry mass, kg	−1450
Nominal SEPS propellant, kg	−1533
Reserves + contingencies propellant, kg	100
Trapped propellant, kg	−20
Net payload, kg	850

Table 7 Mission profile for the Vesta-Roberta-Penelope asteroid tour

Julian date −244,0000	Calendar date	Elapsed time, days	Flight time, days	Event	Propellant drop mass, kg	Mass, kg
7544	1/17/89	0		Launch		3426
			760			
8304	2/16/91	760		Arrive Vesta		2553
			120	Operations at Vesta	50	
8424	6/16/91	880		Depart Vesta		2503
			599			
9023	2/4/93	1479		Arrive Roberta		2226
			50	Operations at Roberta	30	
9073	3/26/93	1529		Depart Roberta		2196
			515			
9588	8/23/94	2044		Arrive Penelope		2047
			100	Operations at Penelope	30	
9688	12/1/94	2144		End of mission		2017

Mass Summary

Two-stage IUS capability at $v_{\infty_0} = 2.986$ km/s, kg	3526
IUS-SEPS adapter, kg	−100
SEPS dry mass, kg	−1450
Nominal SEPS propellant, kg	−1409
Reserves + contingencies propellant, kg	−100
Trapped propellant, kg	−20
Net payload, kg	477

Because of the interaction between successive target trajectories, a complete asteroid tour is necessarily optimized in steps. To facilitate discussion, Fig. 2 defines the notation. A complete tour of four asteroids would be optimized in the following sequence of steps with a rendezvous occurring at each asteroid: $E-A_1$, A_1-A_2, $E-A_1-A_2$, A_2-A_3, $E-A_1-A_2-A_3$, A_3-A_4, $E-A_1-A_2-A_3-A_4$. The beginning mass of each asteroid-asteroid arc is the final mass of the previous step beginning at Earth. In this way, nearly converged sets of $\bar{\lambda}_r$, $\bar{\lambda}_v$ are maintained as successive asteroids are added to the tour. Generally, the stay time at each asteroid was 50 days, and 30 kg of mass simulating maneuvering propellant was dropped at each asteroid. Vesta, the third largest known asteroid, is an exception. Because of its size, longer times for maneuvering are required and 50 kg of maneuvering propellant and 120 days of stay time were allotted. In general, longer stay times decrease the final mass. Interestingly, final mass was an increasing function of final time and so trip times were reasonably picked to give an adequate payload.

When the first tours were obtained, it was discovered that changing launch dates meant duplicating almost all of the work done in finding the tour. The following technique eliminates the problem and works very rapidly for a new launch date. Propagate the initial $(\bar{\lambda}_r, \bar{\lambda}_v)_{t_0}$ along the Earth's Keplerian orbit to the new launch date, $t_0+\Delta t_0$, and obtain

Table 8 Mission profile for the Medusa-Nysa-Erigone-Massalia asteroid tour

Julian date − 244,0000	Calendar date	Elapsed time, days	Flight time, days	Event	Propellant drop mass, kg	Mass, kg
7406	9/1/88	0		Launch		3885
			680			
8086	7/13/90	680		Arrive Medusa		3037
			50	Operations at Medusa	30	
8136	9/1/90	730		Depart Medusa		3007
			677			
8813	7/9/92	1407		Arrive Nysa		2725
			50	Operations at Nysa	30	
8863	8/28/92	1457		Depart Nysa		2695
			454			
9317	11/25/93	1911		Arrive Erigone		2490
			50	Operations at Erigone	30	
9367	1/14/94	1961		Depart Erigone		2460
			291			
9658	11/1/94	2252		Arrive Massalia		2309
			100	Operations at Massalia	30	
9758	2/9/95	2352		End of mission		2279

Mass Summary

Two-stage IUS capability at $v_{\infty_0} = 2.185$ km/s, kg	3985
IUS-SEPS adapter, kg	− 100
SEPS dry mass, kg	− 1450
Nominal SEPS propellant, kg	− 1606
Reserves and contingencies propellant, kg	− 100
Trapped propellant, kg	− 20
Net payload, kg	709

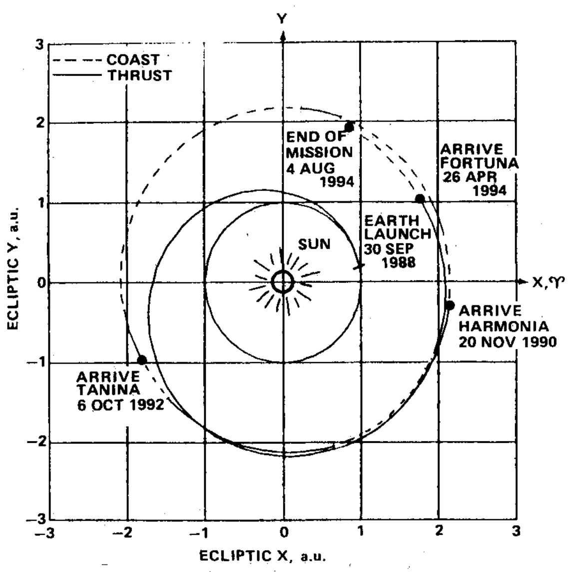

Fig. 4 Harmonia-Tanina-Fortuna asteroid tour.

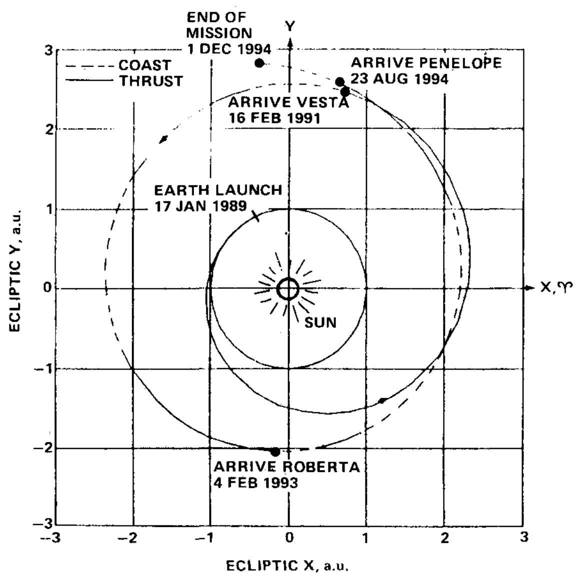

Fig. 5 Vesta-Roberta-Penelope asteroid tour.

$(\bar{\lambda}_r,\bar{\lambda}_v)_{t_0+t_0}$. Assuming the flight time to the first asteroid is t_{flt} for the nominal launch date, use $(\bar{\lambda}_r,\bar{\lambda}_v)_{t_0+\Delta t_0}$ as a starter to rendezvous with the first target in a fixed flight time, $t_{flt} - \Delta t_0$. This easily converged step gives a $(\bar{\lambda}_r,\bar{\lambda}_v)^*_{t_0+\Delta t_0}$ as a starter for the entire tour and also causes easy convergence. This method works very well for Δt_0 up to ± 30 days, primarily because the initializing trajectory for the new launch date is nominal from the first target onward.

The Tours

Tour 1

The first tour visits Eros, Ilona, and Drakonia. Eros is a near-Earth asteroid and the other two are mid-main-belt asteroids. The launch date is Jan. 4, 1988 and the tour is over in 5.4 yr on May 27, 1993. Less than the full solar array output is used on the Eros leg only to ensure satisfaction of the engine lifetime constraint. A maximum array power of 19.2 kW reduces propellant usage sufficiently. Table 5 summarizes the mission profile and Fig. 3 shows the trajectory projected onto the heliocentric ecliptic plane. Excellent Earth viewing is available at each target during stationkeeping maneuvers. For a 300 kg payload, a margin of 306 kg exists.

Tour 2

Harmonia, Tanina, and Fortuna are the subjects of this tour which launches Sept. 30, 1988 and terminates 5.8 yr later

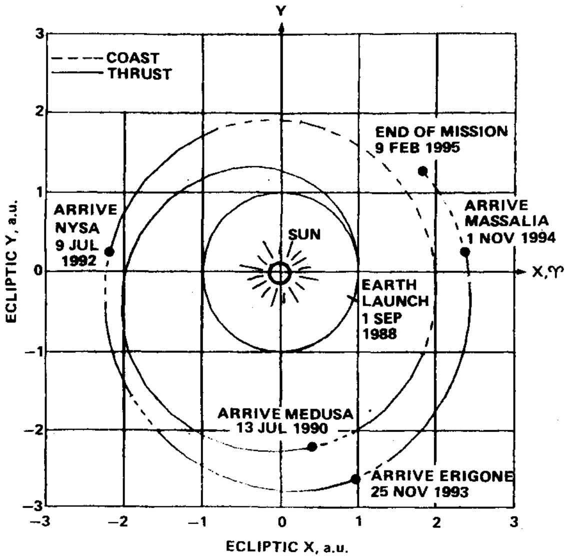

Fig. 6 Medusa-Nysa-Erigone-Massalia asteroid tour.

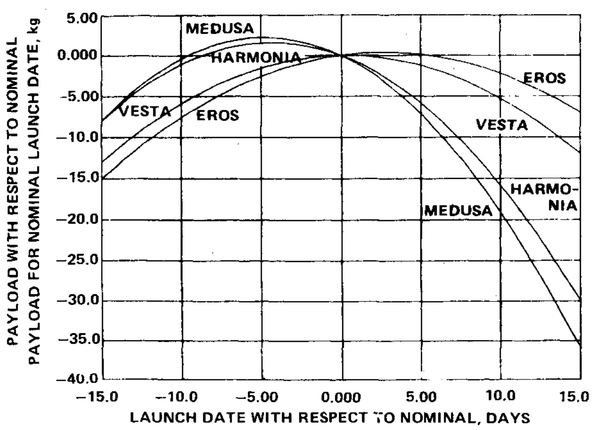

Fig. 7 Launch windows for the four asteroid tours.

on Aug. 4, 1994. Harmonia is an inner main-belt asteroid. In contrast to the other tours, the final payload mass can be increased by longer stay times at Harmonia and Tanina. Table 6 gives the mission profile and Fig. 4 shows the ecliptic plane projection of the trajectory. Unfortunately, a superior conjunction with the sun occurs for Tanina and approximately the first half of the Fortuna rendezvous occurs within 30 deg of the sun. Considering the 550 kg payload margin available, some trajectory shaping is easily possible to improve Earth viewing.

Tour 3

Vesta, Roberta, and Penelope comprise the third tour which launches Jan. 17, 1989 and ends 5.9 yr later on Dec. 1, 1994. Vesta is an important target, being the third largest known asteroid. A mission profile is given in Table 7 and Fig. 5 shows the ecliptic projection of the trajectory. Earth viewing of each asteroid rendezvous is excellent except that the last one-third of the stay time at Vesta occurs within 30 deg of the sun. A payload margin of 147 kg is available.

Tour 4

This tour was included in the industry RFP and was originally developed at JPL. The targets are Medusa, Nysa, Erigone, and Massalia. Launch occurs on Sept. 1, 1988 and the tour ends on Feb. 9, 1995, a duration of about 6.4 yr. Medusa is an example of an optimum first asteroid target because of its nearness, low eccentricity and inclination, and because a large diversified set of asteroid sequences are later accessible. Table 8 gives the mission profile and Fig. 6 shows the ecliptic trajectory projection. Earth viewing is good except that most of the Erigone encounter occurs within 30 deg of the sun. The 409 kg payload margin undoubtedly would allow one or two more targets to be selected.

Tour Launch Windows

Thirty-day launch windows have been obtained for each of the tours. Since payloads were increasing functions of flight times, comparability was obtained by holding flight time constant at its nominal value as launch date was varied. The results are shown in Fig. 7. Unacceptable payload decreases can of course be compensated by small flight-time increases.

Conclusions

It has been shown that the calculus of variations can be successfully applied to define asteroid tours that were previously found by more approximate means. The numerical effort required can be difficult and time consuming, but techniques reducing these concerns have been outlined. The trajectories obtained verify that a SEPS vehicle can deliver significant scientific payloads to a succession of asteroids having diverse characteristics.

References

[1]Duncan, J.C., *Astronomy,* 5th ed., Harper and Brothers, New York, 1955, pp. 273-275.

[2]Alfven, H. and Arrhenius, G., "Mission to an Asteroid," *Science,* Vol. 167, 1970, pp. 139-141.

[3]Gehrels, T., ed., *Physical Studies of Minor Planets,* NASA SP-267, 1971.

[4]Morrison, D. and Wells, W.C., eds., "Asteroids: An Exploration Assessment," NASA CP-2053, 1978.

[5]Friedlander, A.L., Wells, W.C., Davis, D.R., Housen, K., and Wilkening, L.K., "Asteroid Mission Study," Science Applications, Inc., Schaumberg, Ill., SAI-1-120-839,M11, May 1979.

[6]Friedlander, A.L. and Vickers, R.S., "A Survey of Missions to the Asteroids," IIT Research Institute, Chicago, Ill., M-3, 1964.

[7]Friedlander, A.L., "Asteroid (Flora and Eros) Sample-Return Missions via Solar Electric Propulsion," IIT Research Institute, Chicago, Ill., Rept. T-30, 1971.

[8]Bender, D.F., "Ion Drive Multi-Asteroid Rendezvous Trajectories," *Proceedings of the AAS/AIAA Astrodynamics Conference,* Jackson, Wy., Paper 77-3, 1977.

[9]Wright, J.L., "Asteroid Multiple Rendezvous Mission Concept," Jet Propulsion Laboratory, Pasadena, Calif., Rept. No. 710-26, Feb. 1979.

[10]"Planetary Missions Performance Handbook – Vol. III, Comets and Asteroids," Science Applications, Inc., Schaumberg, Ill., Rept. SAI-1-120-275-M15, May 1981.

[11]"Asteroid Exploration Mission (ASTREX). An Assessment Study," European Space Agency, Paris, France, Rept. ESA-SCI (79) 1, Oct. 1979.

[12]Thomson, A.A., "Off to the Asteroids," *Spaceflight,* Vol. 24, Jan. 1982, pp. 7-9.

[13]Yen, C-W.L., "Main Belt Asteroid Exploration – Mission Options for the 1990's," AIAA Paper 82-1463, Aug. 1982.

[14]Heacock, R.L. and Rose, J.R., "Mariner Mark II – An Approach to Solar System Exploration in the 1990's," 33rd International Astronautical Congress, Paris, France, Paper 82-195, Sept. 1982.

[15]"The Asteroid Rendezvous Spacecraft, An Adaptation Study of TIROS/DMSP Technology," RCA Astro-Electronics, Princeton, New Jersey, NASA CR-169909, Dec. 1982.

[16]Meinzer, K., "The AMSAT Mission to the Asteroid Belt," 34th International Astronautical Congress, Budapest, Hungary, Paper 83-207, Oct. 1983.

[17]Yen, C-W.L., "Mission Options for the First SEPS Application – Rendezvous with Near Earth Asteroids and Comets," AIAA Paper 81-186, Aug. 1981.

[18]"Solar Electric Propulsion System (SEPS) Request for Proposal," NASA DCN 8-1-9-PP-00854, July 1979.

[19]Hahn, D.W. and Johnson, F.T., "Final Report for Chebychev Trajectory Optimization Program," The Boeing Co., Seattle, Wash., Rept. D180-12916-1, June 1971.

[20]Friedlander, A.L., "TOURAST Computer Program," Science Applications, Inc., Schaumberg, Ill., 1978.

[21]Friedlander, A.L., Niehoff, J.C., Soldner, J.K., and Wells, W.C., "Multiple Asteroid Tour Identification for 1988-1989 Launches," Science Applications, Inc., Schaumberg, Ill., Rept. SAI-1-120-318-T18, July 1981.

[22]"30-Centimeter Ion Thrust Subsystem Design Manual," NASA TM 79191, June 1979.

[23]Burrows, R.R. and McDaniel, G.A., "A Method of Trajectory Analysis with Multimission Capability and Guidance Application," AIAA Paper 68-844, Aug. 1968.

[24]Fehlberg, E., "Low-Order Classical Runge-Kutta Formulas with Stepsize Control and Their Application to Some Heat Transfer Problems," George C. Marshall Space Flight Center, Huntsville, Ala., NASA TR R-315, July 1969.

[25]Goodyear, W.H., "A General Method for the Computation of Cartesian Coordinates and Partial Derivatives of the Two-Body Problem," International Businekss Machines Corp., Greenbelt, Md., NASA CR-522, Sept. 1966.